

Yu.I. Sementsov<sup>1,2</sup>, Hao Tang<sup>1</sup>, Dongxing Wang<sup>1</sup>, E.M. Demianenko<sup>2</sup>, M.I. Terets<sup>2</sup>,  
K.O. Ivanenko<sup>1,3</sup>, O.M. Ignatenko<sup>2</sup>, S.M. Makhno<sup>1,2</sup>, N.V. Sigareva<sup>2</sup>, S.V. Zhuravskiy<sup>2</sup>,  
Yu.V. Hrebelna<sup>1</sup>, O.A. Cherniuk<sup>2</sup>, M.T. Kartel<sup>2</sup>

## The systems polyethylene and polypropylene – CNTs nanofillers: quantum-chemical modeling and experimental characteristics

<sup>1</sup>Ningbo Sino-Ukrainian New Materials Industrial Technologies Institute, Zhenhai district, Ningbo, China

<sup>2</sup>Chuiko Institute of Surface Chemistry, NAS of Ukraine, Kyiv, Ukraine, [microft2@ukr.net](mailto:microft2@ukr.net)

<sup>3</sup>Institute of Macromolecular Chemistry, NAS of Ukraine, Kyiv, Ukraine

The purpose of this work was to investigate the interaction of graphene-like nanoclusters with fragments of polymers of the same nature, but of a slightly different structure, for example, polyethylene (PE) and polypropylene (PP), experimentally and using quantum chemistry methods. It is experimentally shown that the reinforcement of PE and PP with carbon nanotubes (CNTs) by mixing in the melt, previously distributed from a stable aqueous dispersion on the surface of the polymer powder, leads to a change in structural, mechanical and thermodynamic characteristics. The degree of crystallinity changes, and the coherent scattering domain (CSD) size, the fracture stress increases, the fracture deformation, thermodynamic characteristics change, and such changes in characteristics for the PP-CNTs system prevail in comparison with the PE-CNTs system.

The interaction energy of graphene-like fragments with PE and PP oligomers was calculated. It was established that the energy of interaction of a graphene-like nanocluster with a PP oligomer is greater, compared to PE, which is consistent with experimental data on the melting temperatures of pure polymers and polymer composites with nanotubes. The polymer with the surface of the nanocarbon fragment forms an intermolecular complex that is not covalently bound but is held by intermolecular dispersion forces.

**Keywords:** nanocomposite, carbon nanotube, polyethylene, polypropylene, density functional theory method, dispersion forces of interaction.

Received 24 July 2024; Accepted 25 November 2024.

### Introduction

Composite materials are the most adaptable and advanced engineering materials of the modern world [1]. Currently, polymer nanocomposites are gaining more and more attention among the scientific community due to their different applications in everyday life and are considered as an alternative to conventional composites. Due to the presence of nanosized materials, nanocomposites have a large interfacial area available for stress transfer compared to conventional microcomposites. Therefore, nanocomposites demonstrate new and improved properties compared to pure polymers or their traditional composites [2–4]. These

include improved mechanical, thermal, barrier, fireproof and electrical properties [2–5]. Physics-mechanical characteristics (strength, creep, viscosity, etc.) are one of the most important characteristics of a material that determine its operational properties regardless of its functional purpose. Due to the combination of mechanical, thermal and electrophysical properties inherent in carbon nanotubes (CNTs), there is a constant expansion of the spectrum of not only their application, but also the possibilities of using them for fundamental research. The complex of physical properties of nanotubes makes them ideal fillers for polymer composite materials [6–15]. Today, it is possible to significantly increase the thermal conductivity of matrices and obtain conductive polymers

with a low concentration of CNTs. Such materials are used to create conductive elements, battery electrodes, sensors, protective screens, antistatic and anticorrosive coatings, etc. At the same time, the mechanical properties, namely: the average modulus of elasticity of CNTs is more than 1.8 TPa (the measured value is 1.3 TPa) [16], the tensile strength is 63 GPa [17], putting them in the same row as the most promising reinforcing fillers when creating composite materials with increased mechanical characteristics. However, the propensity of CNTs to form agglomerates under the action of van der Waals forces (0.5 eV/nm) is a limiting factor in realizing the potential of these materials [6, 9–15]. For the effective use of CNTs, it is important to ensure high homogeneity of their distribution in the polymer matrix, which is the subject of the works of many researchers [6–10]. The potential of polymers filled with CNTs is much higher because they have higher mechanical characteristics than the unfilled material.

The results of studying the properties of CNT-polymer nanocomposites showed that the use of nanotubes to fill polymer matrices of various types significantly changes their physical properties compared to the original polymers. However, the effect of CNTs on the properties of the obtained nanocomposites at the molecular level has not been definitively clarified. Since the interaction and properties of polymers with nanotubes are successfully studied by computer modeling methods [18–22]. Therefore, the purpose of this work was to consider the regularities of the influence of carbon nanotubes on the structural, electrical and mechanical characteristics of a composite material based on polymers: polyethylene (PE), polypropylene (PP) experimentally, and to investigate the interaction of CNTs with small-sized oligomers of polymers of different nature using the example of polyethylene and polypropylene methods of quantum chemistry.

## **I. Materials and Methods**

Low-density PE and PP as matrixes and multi-walled carbon nanotubes (CNTs) as fillers were chosen for preparation of polymer nanocomposites samples for testing. The multi-walled carbon nanotubes (Fig. 1) (TU U 24.1-03291669-009:2009 (ISC NAS of Ukraine)) were synthesized using chemical vapour deposition procedure in a rotating reactor. Characteristics of the produced CNTs were: average diameter – between 10 and 20 nm; specific surface area (determined through Ar – adsorption) – between 200 and 400 m<sup>2</sup>/g; bulk density – between 20 and 40 g/dm<sup>3</sup>[23]. The CNTs synthesized by CVD-method are obtained in the form of agglomerates. The CNTs were deagglomerated in a device operating on the simultaneous use of shear deformation and cavitation mixing, with a power of 4–7 kW in an aqueous medium. Into the system, 10 liters of water were poured and 124 g of the initial CNTs, i.e., about 100 g of purified CNTs, were added. The treatment was carried out for 4 minutes. After that, the CNTs were cleaned in the traditional way – with a solution of hydrofluoric acid. After purification, the CNTs were washed to pH 6–7. A mixture of PE or PP powders with an aqueous suspension of CNTs was dried in a screw

evaporator. Polypropylene or polyethylene composites with CNTs were obtained in the form of granules by mixing in a twin-screw extruder, from which samples were also made in the form of films and volumetric cylinders. The concentration of nanotubes was from 0,05 to 5.0 %wt.

X-ray studies were carried out on an automated X-ray diffractometer DRON-3M with radiation  $\lambda_{Co}=0,17902$  nm. The average size of crystallites is calculated using the Scherer formula [25]. Transmission electron microscopy (TEM) (JEM-100 CXII) was used to determine the structural characteristics of CNTs. Investigation of the surface of the initial PE and the nanocomposite PE–CNTs was provided with an atomic force microscope NanoScope IIIa (Veeco Corp.). The obtained data were processed using software GWIDDION. Structural and phase transformations as well as the processes connected with the destruction of polymer composites in air were investigated using differential thermal and gravimetric analyses (DTA, DTG) derivatograph Q 1500 D. Compression or tension tests of the polymeric materials and their composites were performed using tensile machine 2167 P-50 with automatic recording of the deformation diagram on the PC. Measurements were carried out at a load speed of 5 mm/min. The conductivity measurements were carried out by a two-contact method at low frequencies using an E7-14 imitansmeter at room temperature [26].

## **II. Objects and calculation methods**

Using the GAMESS (US) program [27] within the framework of the density functional theory (DFT) with the B3LYP functional [28, 29] and the 6-31G(d,p) basis set, the simulation of the intermolecular complexes of the fragment of the outer surface of multilayer CNT with oligomers was carried out. Oligomers contain one, two and three elementary links, which will be called monomers, dimers and trimers of polyethylene and polypropylene. To take into account the dispersion effects of binding [30, 31], which occur during the formation of non-covalent intermolecular complexes, the Grimme D3 dispersion correction [32, 33] was taken into account in the calculations of the intermolecular interaction energy. The choice of the B3LYP-D3 D-DFT method can be justified by the fact that it is not time-consuming, compared to calculations using the B97D or wB97XD functionals. In addition, according to [34], all three methods give comparable results regarding geometric parameters and binding energy for objects similar to ours. To simplify the calculations, oligomers as elementary units of PE ( $-\text{CH}_2-\text{CH}_2-$ )<sub>n</sub> and PP ( $-\text{CHCH}_3-\text{CH}_2-$ )<sub>n</sub>, where n = 1, 2, 3, were represented by the corresponding saturated hydrocarbons, namely ethane, n-butane and n-hexane (for PE) and propane, 2-methylpentane and 2,4-methylheptane (for PP). As noted, when creating nanocomposites based on PE and PP, multilayer CNTs with an outer diameter of 10 to 20 nm were used. As shown by the results of modeling the cross-section of a nanotube with a diameter of 20 nm, it turned out that when fragments of a small size, for example less than 1 nm (trimers) of selected polymers, interact, the outer surface of the nanotube looks almost without positive curvature of

the cylinder. This allows considering the interaction of small-sized oligomers of these polymers with the outer surface of CNTs as intermolecular complexes of oligomers of selected polymers with a graphene-like plane.

Therefore, a graphene-like plane of 40 carbon atoms was chosen as a model for the outer surface of the CNT, as was done in [18]. In this case, the distance between the most remote carbon atoms in this graphene-like cluster is 1.2 nm. Therefore, to equalize uncompensated valences and to preserve  $sp^2$ -hybridization at carbon atoms, 16 atoms of hydrogen, one to each carbon atom were added to peripheral atoms (see Fig.2(a)). In addition, in order to take into account, the dimensional effect of the surface of the nanotube fragment model on the interaction energy, in addition to the above described, two larger models were used, the general formula  $C_{54}H_{18}$  and  $C_{96}H_{24}$  (Fig. 2(b) and Fig. 2(c)).

Equilibrium spatial structures of reagent molecules and reaction products were found by minimizing the gradient norm to 0.0001 Hartree. The stationary power minima of relative structures are proved by the absence of negative eigenvalues of Hesse' matrices (matrices of force constants) [35].

### III. Results and discussion

#### Calculation results and their discussion

**Examination of the interaction between polyethylene and polypropylene oligomers.** It is known [36–38] that for thermoplastic polymers, the intermolecular binding energy between their structural units correlates with the melting temperature of the corresponding matter. In the study of intermolecular interactions of the fragments of

polymers with the outer surface of carbon nanotubes, magnitudes of the energy of intermolecular interaction of the fragment of polymers of different sizes for polyethylene polymers (Fig. 3 a–c) and polypropylene (Fig. 3 d–f) were estimated (Table 1).

Fig. 3 shows the most probable intermolecular complexes, the total energies of which were minimal. In addition, we have shown that, regardless of the size of the fragment of polymers of polyethylene and polypropylene (Table 2), the average distance between the carbon atoms is about 0.390 nm, which indicates the absence of chemical bonding between different oligomers [37].

The results of the analysis of calculations (see Table 1) demonstrate that the energies of interaction between two identical monomers are  $-8.0$  kJ/mol and  $-14.4$  kJ/mol, respectively for PE and PP. With an increase in the size of the oligomeric units to two ( $n = 2$ ) for each of the polymers, the energy of their interaction is also almost twice as high, while the energy is  $-20.3$  and  $-25.9$  kJ/mol, respectively. By further increasing the size of studied oligomers ( $n = 3$ ), the energy of the intermolecular interaction also increases:  $-32.9$  kJ/mol for PE and  $-40.6$  kJ/mol for PP. In this case, for a linear chain of polyethylene, an increase in the length of the fragments that interact with each other results in a monotonic decrease in the distance between the oligomers (0.390, 0.382, 0.378 nm). This is also consistent with the energy of interaction per number of elemental links of the polymer. In particular, for the complex consisting two double-polymer units to find out this value, it is necessary to divide  $-20.3$  kJ/mol into two and we so obtain the value of  $-10.2$  kJ/mol, which is 2 kJ/mol less than the similar value for a complex of double monomer parts of PE ( $-8.0$  kJ/mol). For the complex consisting of two trimers

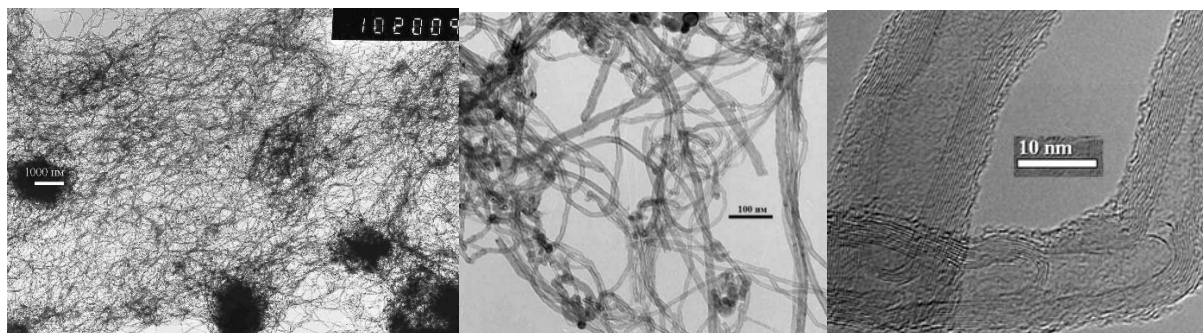


Fig. 1. TEM images of MWCNTs obtained on Fe-Al-Mo-O catalyst.

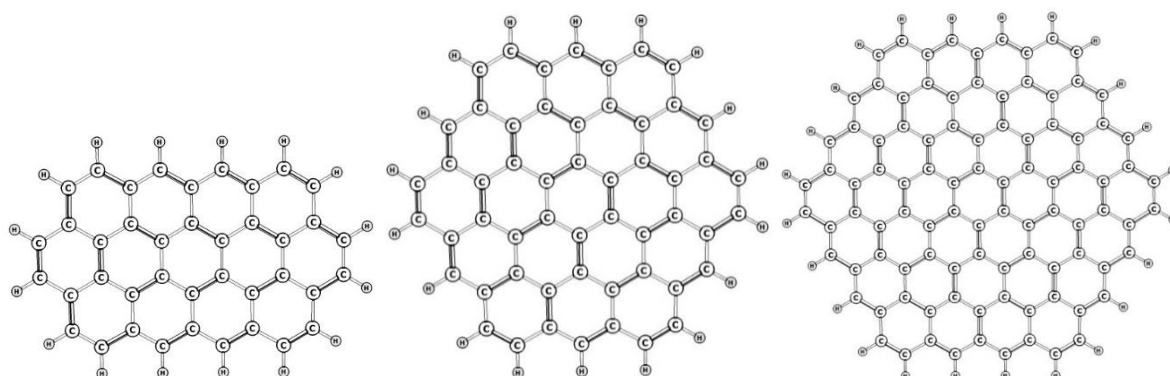


Fig.2. Models for the fragment of the outer surface of CNT by the general composition: (a)  $C_{40}H_{16}$ ; (b)  $C_{54}H_{18}$ ; (c)  $C_{96}H_{24}$ .

(Fig.3(c)), this value is even larger and is divided into three ( $-33.0/3 = -11.0$  kJ/mol).

For PP, a similar trend of change in distance is not observed. The energy of intermolecular interaction per one elementary PP link also does not increase with an increase in the number of elementary units: compared to the complex consisting of PP monomers and having the intermolecular interaction energy value of  $-14.4$  kJ/mol. For a link consisting of two elementary units, this value is  $-25.9/2 = -13.0$  kJ/mol and for the trimeric PP fragment  $-40.6/3 = -13.5$  kJ/mol, respectively. This can be explained by the fact that PP has a more complex structure (the presence of a methyl group in each elementary chain), in comparison with PE. Thus, with an increase in the number of elemental units in PP oligomer, the energy per PP unit does not differ significantly; it equals not more 3 kJ/mol. Therefore, for the study of intermolecular interaction between individual groups of polymeric units, it is enough to use oligomers consisting of two or three elementary units.

Consequently, based on the analysis of the calculation results, it can be argued that, regardless of the size of the fragments of these polymers, comparing the value of intermolecular energy for the same number of elementary units of these two polymers, the PP fragments are more tightly bound than those of PE, which means that in order to disconnect the PP links, which are connected by non-covalent bonds, more energy is needed than for PE. The calculation results obtained are consistent with experimental data on the melting temperature of polymers, since the melting temperature of PE is  $120^{\circ}\text{C}$ – $140^{\circ}\text{C}$ , and for PP this value is higher ( $130^{\circ}\text{C}$  to  $170^{\circ}\text{C}$  as dependent on the polymer grade [39, 40]).

**Interaction of fragments of a carbon nanotube with polyethylene oligomers.** In connection with the choice of a graphene-like plane as a fragment of the outer surface of CNT interacting with PE oligomers, it is crucially important to confirm the reliability of the calculated energy values of intermolecular interaction. Therefore, intermolecular complexes with different amounts of

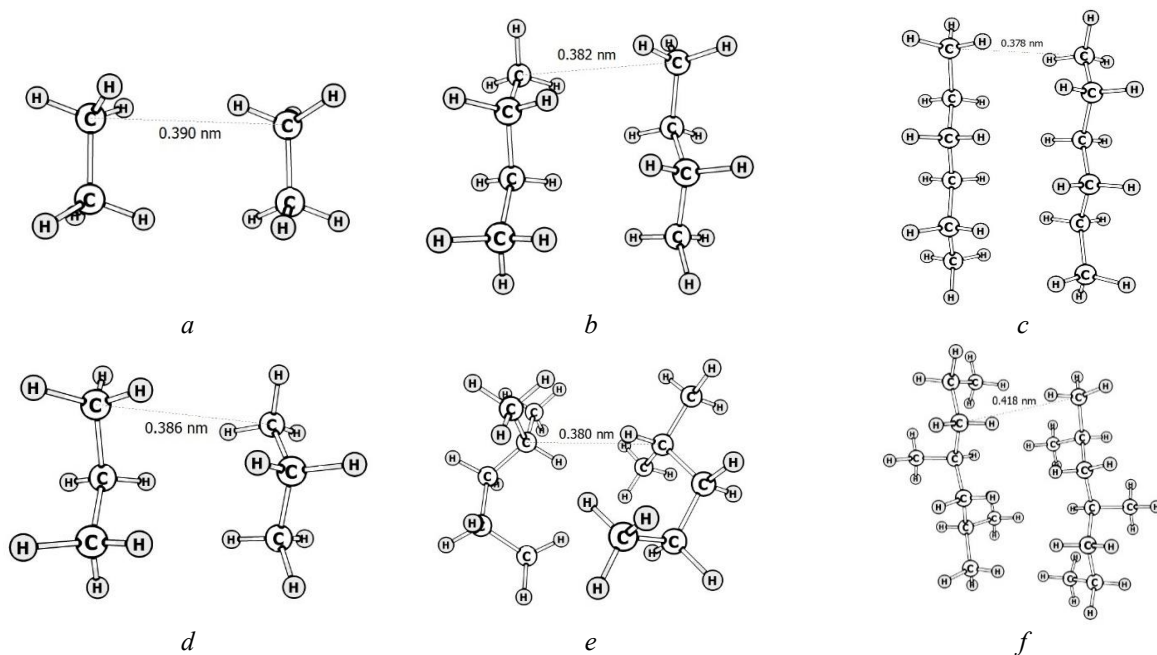


Fig. 3. The most probable intermolecular complexes of polyethylene oligomers (a–c) and polypropylene (d–f).

Table 1.

Intermolecular binding energy values for pure polymers and nanocomposites (kJ/mol)

Number links in the oligomer	Pure polymers		Nanocomposites					
	Polyethylene	Polypropylene	Polyethylene			Polypropylene		
			C <sub>40</sub> H <sub>16</sub>	C <sub>54</sub> H <sub>18</sub>	C <sub>96</sub> H <sub>24</sub>	C <sub>40</sub> H <sub>16</sub>	C <sub>54</sub> H <sub>18</sub>	C <sub>96</sub> H <sub>24</sub>
1	-8.0	-14.4	-31.5	-30.0	-33.0	-41.3	-45.1	-46.3
2	-20.3	-26.0	-54.6	-56.4	-57.4	-66.4	-69.3	-71.0
3	-33.0	-40.6	-80.5	-80.6	-81.3	-87.6	-89.2	-92.1

Table 2.

Intermolecular distances values for pure polymers and nanocomposites (nm)

Number links in the oligomer	Pure polymers		Nanocomposites					
	Polyethylene	Polypropylene	Polyethylene			Polypropylene		
			C <sub>40</sub> H <sub>16</sub>	C <sub>54</sub> H <sub>18</sub>	C <sub>96</sub> H <sub>24</sub>	C <sub>40</sub> H <sub>16</sub>	C <sub>54</sub> H <sub>18</sub>	C <sub>96</sub> H <sub>24</sub>
1	0.390	0.386	0.329	0.346	0.329	0.344	0.344	0.339
2	0.382	0.380	0.345	0.343	0.342	0.339	0.340	0.343
3	0.378	0.418	0.342	0.339	0.341	0.344	0.349	0.342

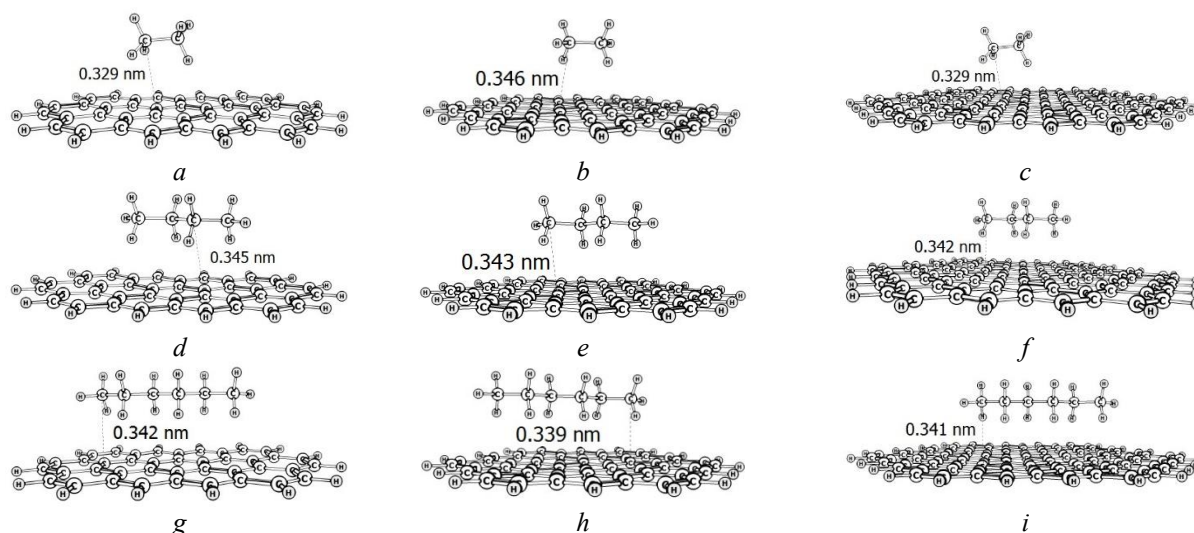


**Fig. 4.** The structure of different length of polyethylene fragments in intermolecular complexes with graphene-like clusters of different sizes, modeling a fragment of the outer surface of a carbon nanotube.

polymeric units (1, 2, 3) and graphene-shaped planes of various sizes ( $C_{40}H_{16}$ ,  $C_{54}H_{18}$ , and  $C_{96}H_{24}$ ) were modeled (Fig. 4).

For complexes where the fragment of the outer surface of CNT has the smallest graphene cluster  $C_{40}H_{16}$ , the intermolecular distance between of the fragment of polymers and the graphene-shaped plane increases slightly from 0.329 to 0.345 nm with an increase in the size of the fragment of polymers from monomer to dimer, and for the trimer this value is slightly reduced to 0.342 nm. The energy of the intermolecular interaction of the PE monomer with the graphene plane is  $-31.5$  kJ/mol, for dimer this value is  $-54.6$  kJ/mol, and for the trimer  $-80.4$  kJ/mol (Table 1). For intermolecular complexes with the graphene-like cluster  $C_{54}H_{18}$  a tendency arises to shortening intermolecular distance due to an increase in the size of the PE fragments (0.346 nm for the monomer, 0.343 nm for the dimer, and 0.339 nm for the trimer).

The energy of the intermolecular interaction between the PE monomer and the  $C_{54}H_{18}$  cluster is  $-30.0$  kJ/mol, which is 1.5 kJ/mol less than the value for the complex with the  $C_{40}H_{16}$  cluster. For dimer, this value is  $-56.4$  kJ/mol, that is, the energy per polymeric link is slightly smaller than the value for the monomer ( $-28.2$  kJ/mol). When using as a fragment of the outer surface of CNT as a graphene-like cluster of  $C_{96}H_{24}$  composition, there is no similar tendency in shortening the distance compared to the length of the oligomeric chain in previous case with the  $C_{54}H_{18}$  cluster. For PE monomer complex the intermolecular distance is the smallest (0.329 nm), and is similar to that in the complex monomer of PE with  $C_{40}H_{16}$ , unlike that for the complex with dimer. The energies of intermolecular interaction are  $-33.0$ ,  $-57.4$  and  $-81.3$  kJ/mol, correspondingly for monomer, dimer and trimer (Table 1).

Comparing the distances between the carbon atoms for the complexes between two identical oligomers (Fig. 3) and the distance between the graphene planes and the carbon atoms of PE fragments (Fig. 4), it is seen that, regardless of the size of the graphene cluster, this distance is approximately 0.05 nm smaller than similar value for the complexes consisting of two fragments of PE.

**Interaction of a fragment of a carbonnanotube with polypropylene oligomers.** In the study of the interaction of PP oligomers with fragments of the outer surface of CNT, the same three graphene-like clusters were used, as for oligomers of PE with CNT. These intermolecular complexes are depicted in Fig. 5.

For complexes of PP monomer with graphene-like clusters of different sizes the distance between the carbon atoms of the monomer and the graphene-like plane almost does not change, in contrast to the similar value for the complex with PE, and make up 0.340 nm. This is probably due to the larger size of the monomer of PP compared with PE. The energy of the intermolecular interaction for the monomer with the smallest carbon cluster ( $C_{40}H_{16}$ ) is  $-41.3$  kJ/mol. Increasing the size of the cluster to  $C_{54}H_{18}$  results in an increase in the energy of the interaction, which in this case has a value of  $-45.0$  kJ/mol, and a further increase in the size of the graphene-like plane to  $C_{96}H_{24}$  increases to  $-46.3$  kJ/mol (Table 1).

Considering the interaction of graphene-like clusters of different sizes with a two-link PP oligomer, it can be seen that increasing the size of the carbon cluster increases the intermolecular distance from 0.339 nm for the  $C_{40}H_{16}$  cluster to 0.340 nm for  $C_{54}H_{18}$  and 0.343 nm for  $C_{96}H_{24}$ . This distance is almost the same as for a complex with a monomer.

The energy of intermolecular interaction for a complex with the smallest graphene-like cluster and dimer is  $-66.4$  kJ/mol, and for the dimer oligomer of PP with a larger cluster ( $C_{54}H_{18}$ ), the interaction energy is  $-69.3$  kJ/mol. The energy of the interaction of dimer with a graphene-like cluster of maximum size  $C_{96}H_{24}$  has an even greater absolute value of  $-71.0$  kJ/mol (Table 1).

With an increase in the size of the graphene-like cluster up to  $C_{54}H_{18}$  for a complex with a trimer, the binding energy of 1.6 kJ/mol is greater than that for trimer and  $C_{40}H_{16}$  ( $-89.2$  kJ/mol), which is not consistent with the fact of increasing the intermolecular distance in these complexes (see Fig. 4(g) and Fig. 4(h)). Using the maximum size of the  $C_{96}H_{24}$  cluster in the intermolecular complex with the trimer slightly increases the energy of the intermolecular interaction ( $-92.1$  kJ/mol) compared



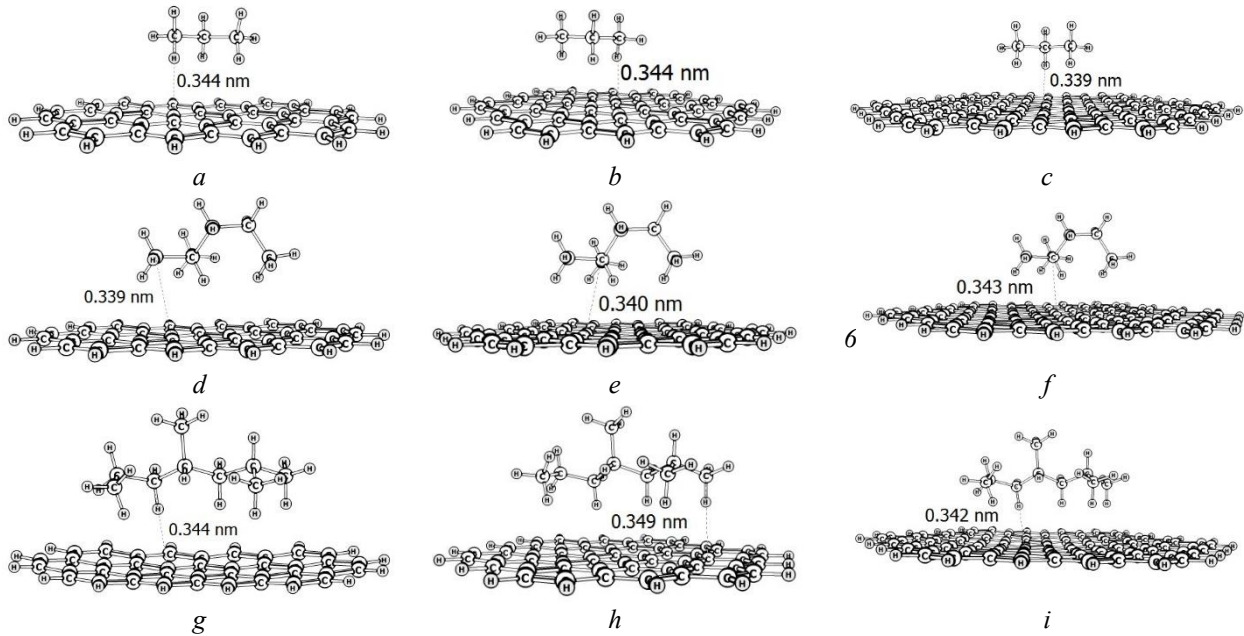


**Fig. 5.** The structure of different length polypropylene fragments in intermolecular complexes with graphene-like clusters of different sizes, which simulate a fragment of the outer surface of a carbon nanotube.

with those for smaller clusters ( $C_{40}H_{16}$  and  $C_{54}H_{18}$ ).

The summary Table 1 shows the numerical values of intermolecular binding energy between two identical oligomers for PE and PP, as well as for their complexes with graphene-like clusters of different sizes. Comparing these data (Table 1), it can be seen that regardless of the size of the graphene-like clusters, the intermolecular interaction between the graphene-like cluster and polyethylene and polypropylene fragments is greater than for a pair of these fragments with each other. Thus, it can be argued that the introduction of carbon nanotubes into polyethylene or polypropylene should increase the strength and melting point of the resulting nanocomposites compared to pure polymers. Table 1 also shows that for pure polymers and their nanocomposites (CNT-polymer), the energy of intermolecular interaction is higher for polypropylene than for polyethylene.

## IV. Experiments Results and Discussion

### Structural features of polymer nanocomposites

The Fig. 6 shows the data of X-ray diffraction, and in table. 3 the crystallinity degree ( $\chi$ ) and size of X-ray coherent scattering blocks (D) of PE-CNTs, PP-CNTs, systems from nanofillers concentration depending on the CNTs concentration were calculated from the X-ray reflex profile.

The adding of CNTs into the polymer matrix demonstrates the structural-forming properties of CNTs. This is observed from a non-monotonic change in the degree of crystallinity depending and CDS size on the concentration of CNTs (Table 3) and atomic force microscopy images (Fig. 7).

These results are in good agreement with the data [12, 24, 41–43], where it was shown that the crystallization of the polymer under shear deformation in the presence of single, five, and multiwall CNTs leads to a change in the

structure of the matrix. For the PE-CNTs system, the distances between the crystal planes (110) and (200) are smaller than the interplane distances in the PE control sample (which is consistent with the data in Table 2), and the polymer chains are oriented along the CNTs axis. The same result (increase in the degree of crystallinity) is observed for the PP-CNTs system, however, in a very narrow range of CNTs concentration up to 0.05 % wt. from 70.0 to 71.8 % wt. Introduction of 0.1 % wt. CNTs reduces the degree of crystallinity to 61 %, followed by an increase in the concentration of CNTs to 5 % wt.

**Electrical conductivity of filled polymers.** The addition of carbon nanotubes to PE and PP polymer matrices causes electrical conductivity, the dependence of which on the filler content is most often described by the percolation theory [44, 45]. It considers the probability of formation of clusters of particles in contact with each other. The description of the critical electric current flow in composite materials (CM) is given by means of the percolation problem formulated for a continuous medium. According to this problem, each point of space with probability  $p = \theta_f$  corresponds to conductivity  $\sigma = \sigma_f$  and with probability  $(1-p)$  – conductivity  $\sigma = \sigma_m$ . The threshold in the percolation terms means the filler concentration at which the phase transition of the second kind of dielectric-conductor occurs. In this case, in the composite system, the regions with high conductivity occupy a minimum fraction of the space –  $\theta_f$ . At small  $p$ , all conductive elements are contained in the isolated clusters of finite size. With increasing  $p$ , the average size of clusters increases and at  $p = \theta_f$ , a through conduction channel, that is, a continuous grid of conducting clusters, appears in the system for the first time. At high  $p$  values, nonconducting regions may already be isolated from each other. Based on percolation theory, the following expressions are obtained to describe the dependence of electrical conductivity on the filler concentration [44, 45]:

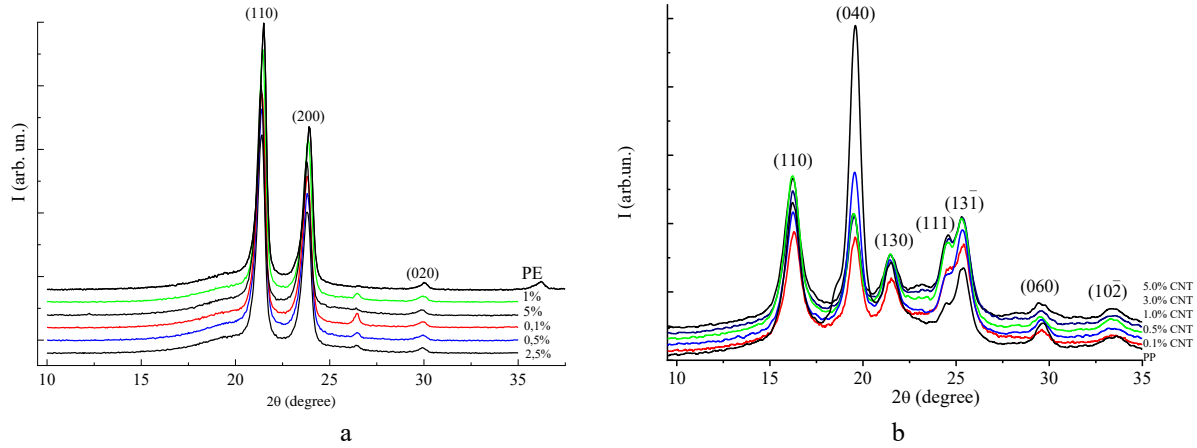


Fig. 6. X-ray diffraction of PE–CNTs (a), PP–CNTs (b).

Table 3.

The crystallinity degree ( $\chi$ ), size of X-ray coherent scattering blocks (D) of PE–CNTs, PP–CNTs, systems from nanofillers concentration

System	Concentration CNTs, % wt.								
	0	0.05	0.1	0.25	0.5	1	2.5	3	5
PE–CNTs, D, nm	21.92	-	19.28	20.5	21.04	21.46	20.12	-	21.35
PE–CNTs, Degree of crystallinity ( $\chi$ ), %	85.6		85.1	79.5	82.8	83.8	81.4		82.3
PP–CNTs, D, nm	11.97	13.01	11.24	-	10.85	10.40	-	10.32	10.27
PP–CNTs, Degree of crystallinity ( $\chi$ ), %	70.9	71.8	60.9	-	63.5	63.8	-	64.0	68.0

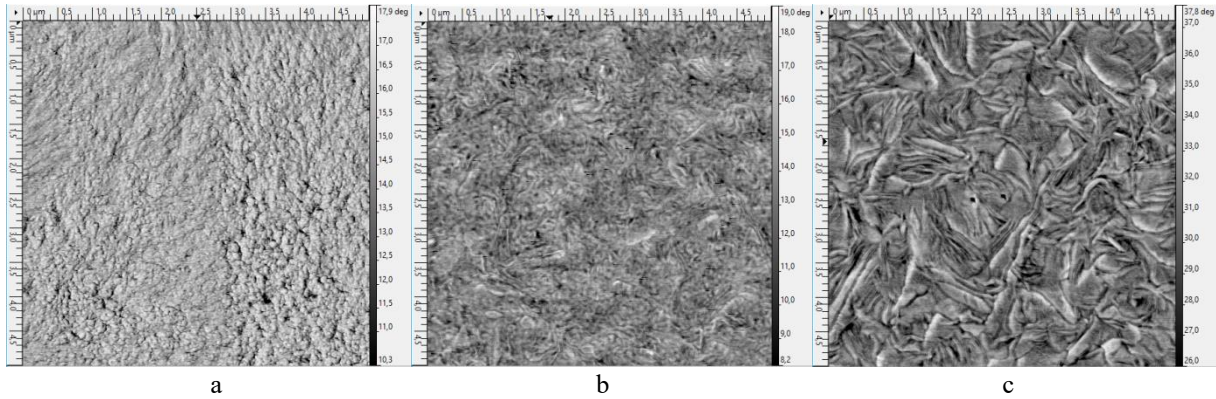


Fig. 7. AFM images of the surfaces of the PE–CNTs composite: pure PE (a), PE–CNT 0.5% wt. (b), and PE–CNT 5.0 % wt. (c).

$$\begin{aligned} \sigma &\sim \sigma_F (\theta - \theta_F)^t, \theta > \theta_F, \\ \sigma &\sim \sigma_m (\theta_F - \theta)^q, \theta < \theta_F, \end{aligned} \quad (1)$$

where  $t, q$  – critical indices of percolation theory.

For three-dimensional model of a composite materials with the spherical filler particles in the percolation theory, the following values of the threshold and critical indices are obtained:  $\theta_F = 17\%$  vol.,  $t = 1,6...1.9, q = 1$ . In practice, significant deviations from the theoretically calculated values are possible. For example, for the graphite-polystyrene system [46]  $\theta_F = 2\%$  vol.,  $t = 0.35$ ; for the carbon black–polyvinyl chloride system, the authors [47] obtained  $\theta_F = 11\%$  wt., the authors [48] –  $9...9.5\%$  wt. at  $t = 1.9 \pm 0.2$ , and the authors [49] for the PE–CNTs system obtained the value  $\theta_F = 0.07\%$  wt. at  $t = 2.1$ .

The dependence of the electrical conductivity on the concentration of CNTs for the studied systems is shown in Fig. 8. The jump in a conductivity in the transition to a

composition with a concentration of 5 % wt. is almost seven orders of magnitude for PE–CNTs (Fig. 8 a) and nine orders for PP–CNTs (8, b). Of course, to create a continuous conductive grid in the polymer matrix, the size of the filler (the length of the CNTs agglomerates) and its distribution in the matrix are of great importance.

Approximating the experimental curves (Fig. 8) and given the linear dependence of the  $\lg \sigma - \lg(\theta - \theta_F)$ , percolation parameters for the both systems were determined. The percolation threshold for the PE–CNTs system was  $(0.45 \pm 0.02)\%$  vol. In this case, the value of electrical conductivity is  $\approx 1.1 \cdot 10^3 (\Omega \cdot \text{m} \cdot \text{cm})^{-1}$ , and the critical index is  $t \sim 1.8$ , corresponding to the three-dimensional system. The calculation of critical indices for the system PP–CNTs gives the following values: -  $\theta_F = 0.345\%$  vol.,  $t = 1.83$ . Deterioration of the homogeneity of the distribution of CNTs (curves 2, 1 Fig. 8b) corresponds to an increase in the critical concentration (percolation threshold) in the range of

0.345 % vol., 0.92 % vol., 1.28 % vol. Therefore, the value of the critical CNTs concentration can be used as a parameter to determine the degree of the homogeneity of filled polymer systems.

Analysis of the results on the electrical conductivity of the obtained systems indicates a significant role of the polymer particle size in the formation of the conductive clusters. This is due to the CNTs distribution in the polymer matrix provided that the polymer particles have a much larger size than CNTs agglomerates [12]. Due to mechanical mixing, the filler covers the surface of the polymer particles, and during hot pressing this structure changes little and the filler remains at the boundary of the polymer particles. Therefore, a cluster conductive structure with a concentration of CNTs above the average and a system of cells with a lower concentration of CNTs or their absence can be formed. In this case, the PE-CNTs system has a sufficiently low percolation threshold and a relatively low influence of the CNTs agglomerate size on the percolation properties of the systems [12].

**The mechanical characteristics of the nanocomposites.** The tests of tensile (Fig. 9 a) and compression (Fig. 9 b) showed that the addition of CNTs changes the mechanical characteristics of the considered composite systems. The dependence of elongation relative to tension stress (Fig. 9 a) for the PE-CNTs system can be divided into four regions: the region with positive curvature in the range up to 5% of deformation for

composites (it may be due to the presence of pores (nanoscale), which work as elastic deformation elements [50]), elastic, plastic regions and fracture of the samples.

Thus, the addition of nanotubes in the polymer matrix, leads to a change in the limit of the tensile strength (increase. Fig. 10), modulus of elasticity (120–213 MPa, Fig. 11), the conditional yield strength (increase by ~50–60 %) and to a significant expansion of the area of plastic deformation of the material. It increases of the destruction deformation from 8% to almost 40%), it means the increases of the work of fracture or fracture energy (area under the curve of deformation).

Note, that the dependences of strength characteristics on the concentration of nanotubes are not monotonous (Fig. 10–11 a, b). Theoretical analysis carried out in various models, for example, [10, 11, 51–53], shows that such a change in properties is due to the characteristics of the different phases formed at the interface of the nanofiller and bulk polymer. The molecular dynamics modelling [10] demonstrates the formation of an ordered polymer matrix layer around the CNTs. This layer, known as the interfacial, plays a central role in the overall mechanical response of the composite.

In the case of «poor» load transfer from the matrix to the CNTs, the effect of reinforcement the CNTs composite is insignificant. Therefore, the presence of an interfacial surface is considered, as the only reason for the enhancement of the composite characteristics. If this

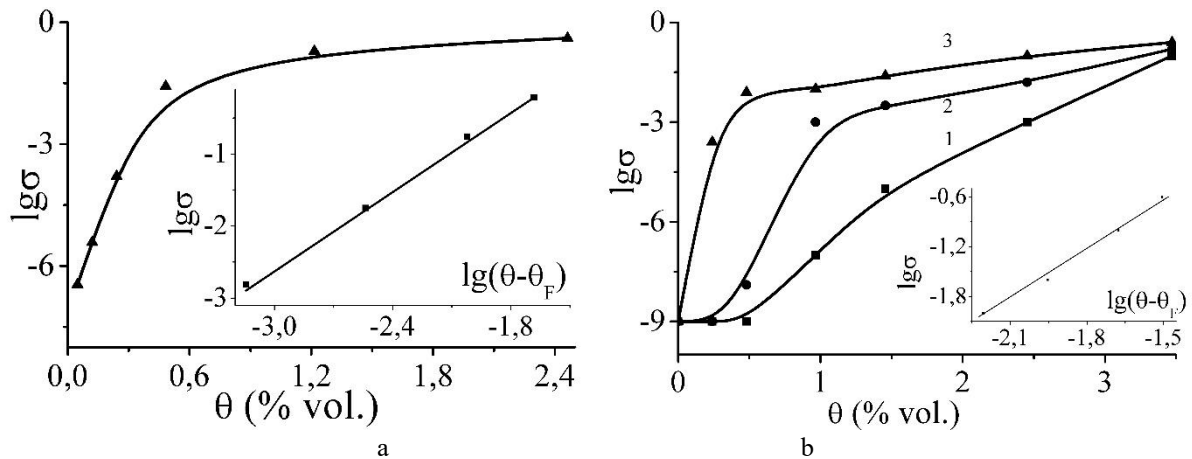


Fig. 8. Dependence of electrical conductivity of PE-CNTs (a), PP-CNTs (b) systems on the concentration of CNTs and linear dependence  $lg\sigma \sim lg(\theta - \theta_F)$  (insert).

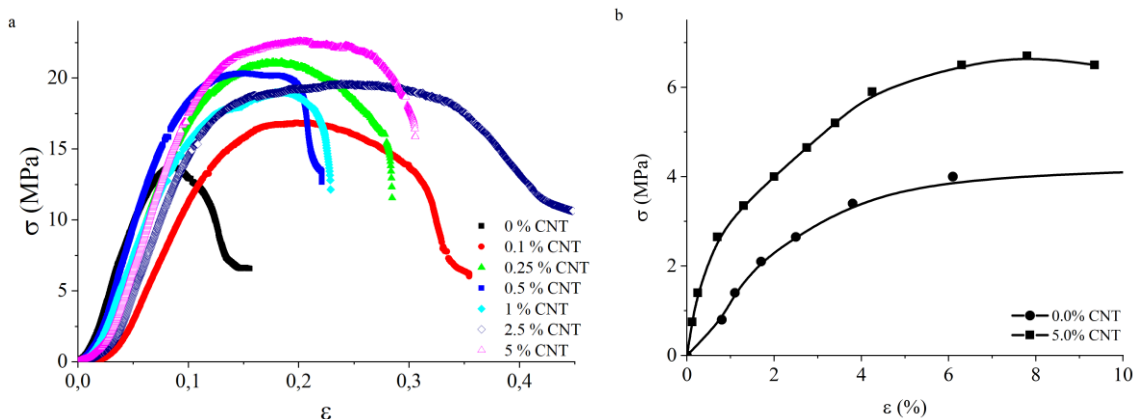
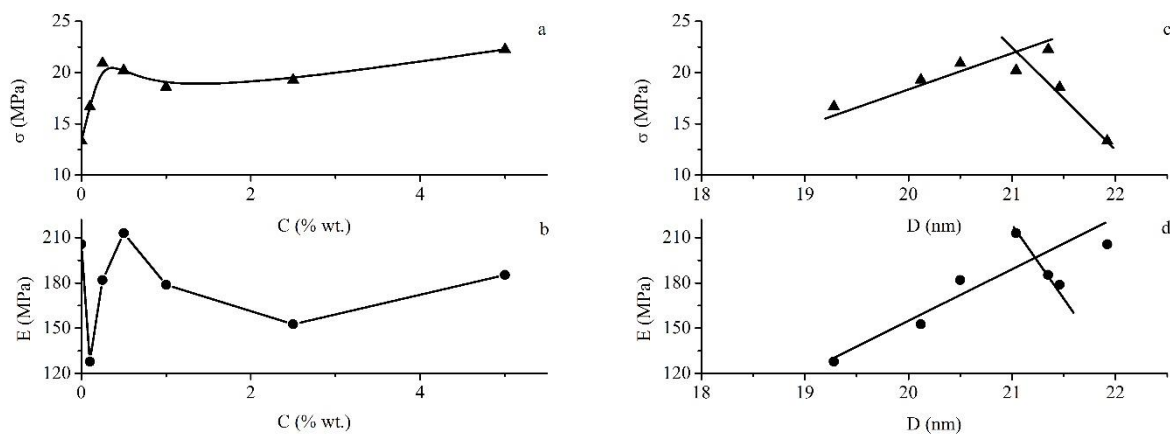
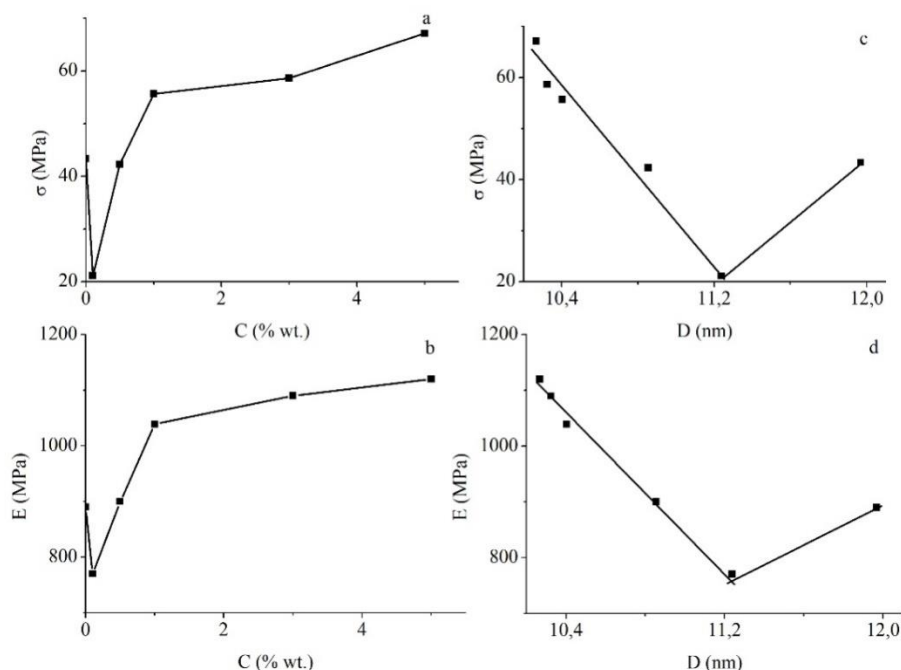


Fig. 9. The dependence of the relative elongation vs tensile stress for the samples of PE-CNTs - (a) and vs compression stress for samples PP-0.1 % wt. CNTs system.





**Fig. 10.** Dependences of the conditional yield strength of composites PE-CNTs (a, c) and the modulus of elasticity (b, d) on the concentration of CNTs (a, b) and the size of the X-ray coherent scattering blocks (c, d).



**Fig. 11.** Dependences of fracture stress by compression of PP-CNTs composites (a, c) and modulus of elasticity (b, d) on CNTs concentration (a, b) and size of the X-ray coherent scattering blocks (c, d).

approach is correct, it is possible to determine experimentally some structural parameter of the system that would characterize the interfacial surface and show a monotonic change in the strength characteristics of the composite from such a parameter.

For polymeric materials, the parameter that reflects the influence of CNTs on the structural hierarchy of the matrix can be, for example, the size of the coherent X-ray scattering block or the degree of crystallinity [10, 11, 53]. The average crystallite size is calculated by Scherer's formula [25].

On Fig. 9 c, d is shown the dependences of the conditional yield strength and elasticity modulus on the value of the CSB for PE-CNTs systems. Fig. 10 c, d is shown the dependences of the compressive strength and elastic modulus on the value of CDS for PP-CNTs systems. For all the above the strength characteristics dependencies on the size of the CDS are linear and are divided into two regions. The boundary between which is

obviously the percolation threshold. For example, for a PE-CNTs system, the CDS size is  $D \sim 21$  nm, which corresponds to a CNTs concentration of  $\sim 0.5\%$  vol. and is in good agreement with the percolation threshold determined from the dependence of the conductivity on the CNTs concentration [54]. Similar results are observed for PP-CNTs. The proposed approach is valid in the field of small CNTs concentration.

**The result of DT analysis of the nanocomposites.**

Fig. 12 a, b shows differential thermal analysis curves for PP-CNTs and PE-CNTs systems, respectively.

From the dependences shown in Fig. 12 a, it follows that a low concentration of CNTs (0.5% wt. %) leads to an increase in the content of the crystalline phase, and a high concentration (5% wt. %) leads to an increase in the disordered component in the composition. At a virtually constant melting point for all compositions, the oxidation temperature of low- and high-molecular fragments for the PP-0.5% wt. CNT composite increases and the process

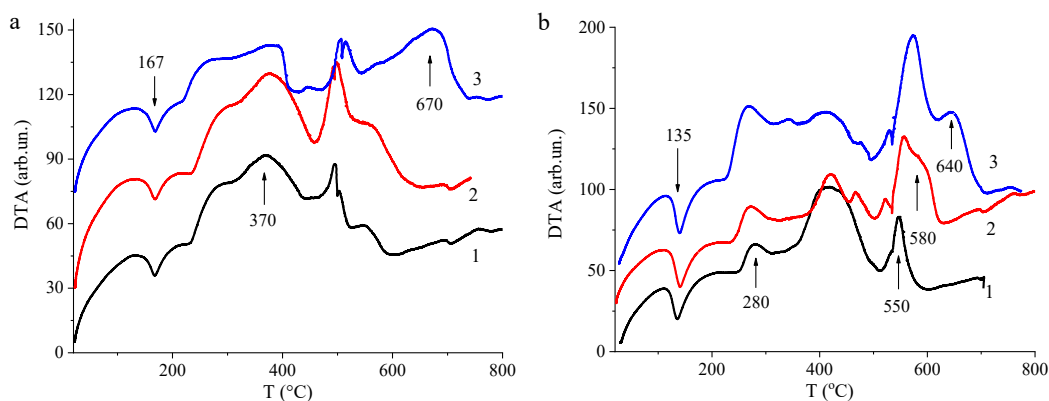


**Fig. 12.** DT analysis curves for: a - the PP-CNTs system with CNTs content, % wt.: 1 – 0, 2 - 0.5, 3 - 5.0; b - the PE-CNTs system with CNTs content, % wt.: 1 – 0, 2 – 2, 3 – 4.

energy (area under the DTA curve) increases. For the PP-5% wt. CNT system, the opposite process is observed. The temperature of the final thermo-oxidative destruction of carbonized polymer and CNT residues and the process energy are higher the higher the CNT concentration.

Fig. 12 b shows that the temperature of the endothermic melting peak of the polymer does not depend linearly on the content of CNTs and may indicate both a change in the crystallinity of PE and the thermal conductivity of the composite as a whole. The second exothermic peak, which characterizes the removal of low molecular weight fractions from the polymer, shifts to the low temperature region by almost 20°C when the content of CNTs increases to 4%. That is, the introduction of a significant amount of CNTs into the polymer can provoke an increase in low molecular weight fragments in the polymer. The temperature of the next peak of thermo-oxidative degradation of the polymer increases with an increase in the content of CNTs to 2% by almost 60°C, but the total contribution to the energy of this process decreases. With an increase in the content of CNTs to 4%, the conversion temperature decreases and the energy contribution increases. With a further increase in temperature, endothermic peaks are observed at approximately the same temperature for all compositions. The DTA curves end with an exothermic peak, which increases and bifurcates into a high-temperature region with an increase in the content of CNTs, which characterizes an increase in the temperature of destruction of polymer and CNT residues.

## Conclusions

The results of quantum chemical modeling have shown that the addition of CNTs to PE and PP increases the energy of intermolecular interaction of polymer-CNTs. For the polymer-CNT complexes, the energy is higher by 18.9 kJ/mol for PE and by 22.5 kJ/mol for PP compared to pure polymers. The polymer fragment with the outer surface of the CNT forms an intermolecular complex that is not covalently bound and is held by intermolecular dispersion forces. The oligomers of polymeric substances and the surfaces of nanotubes in the formed nanocomposites are located closer to each other than the individual polymeric links between them. The energy of

interaction of a CNT fragment with polypropylene oligomers is much higher than with PE.

The simulation results are in qualitative agreement with the experimental results obtained, which showed that the addition of a small amount of nanofillers - multiwalled CNTs ( $\leq 0.5\%$  wt.) into the polymer matrix (PE, PP) significantly changes the structural characteristics of both composites, namely, the degree of crystallinity and the size of coherent X-ray scattering blocks increase until a continuous bulk grid is formed, i.e., the flow threshold is reached. This corresponds to a slight increase in the melting point, which is higher for the PP-CNT system.

The oxidation temperature of low- and high-molecular weight fragments at a low content of CNTs in polymer matrices increases, and the process energy (area under the DTA curve) increases. The opposite process is observed at a CNT content of more than 0.5% wt. The temperature of the final thermo-oxidative destruction of carbonized polymer and CNT residues and the process energy are higher the higher the CNT content.

**Sementsov Yu.I.** – Doctor of Science, Leading Researcher;

**Hao Tang** – Senior Lecturer, Deputy Director, Doctor of Philosophy, Senior Lecturer;

**Dongxing Wang** Lecturer, Doctor of Philosophy, Junior Researcher;

**Demianenko E.M.** – Senior Research Scientist, Candidate of Chemical Sciences;

**Terets M.I.** – researcher, PhD;

**Ivanenko K.O.** – Senior Research Scientist, Candidate of Physical and Mathematical Sciences, Research Scientist;

**Ignatenko O.M.** – Lead Engineer;

**Makhno S.M.** – Head of the Laboratory, Doctor of Physical and Mathematical Sciences, Senior Research Scientist;

**Sigareva N.V.** – researcher, PhD;

**Zhuravskiy S.V.** – researcher, PhD;

**Yu.V. Hrebelna** – junior researcher, Doctor of Philosophy;

**Cherniuk O.A.** – Lead Engineer; Doctor of Philosophy;

**Kartel M.T.** – Academician of NAS of Ukraine, Professor Doctor of Chemical Sciences.

- [1] Y. Shi, Yu. Hrebelsna, E. Demianenko, S. Makhno, K. Ivanenko, S. Hamamda, M. Terets, M. Kartel, Y. Sementsov. *The Carbon Nanotubes, Graphene Nanoparticles Their Oxygen Modified Forms and Composites*. In: Hamamda, S., Zahaf, A., Sementsov, Y., Nedilko, S., Ivanenko, K. (eds) Proceedings of the 2nd International Conference of Nanotechnology for Environmental Protection and Clean Energy Production. ICNEP 2023. Springer Proceedings in Materials. 45, 29 (2024); [https://doi.org/10.1007/978-981-97-1916-7\\_3](https://doi.org/10.1007/978-981-97-1916-7_3).
- [2] A.S. Sethulekshmi, A. Saritha, K. Joseph, *A comprehensive review on the recent advancements in natural updates rubber nanocomposites*, International Journal of Biological Macromolecules 194, 819 (2022); <https://doi.org/10.1016/j.ijbiomac.2021.11.134>.
- [3] J.S. Jayan, A. Saritha, K. Joseph, *MoS<sub>2</sub>: advanced nanofiller for reinforcing polymer matrix*, Phys. E Low Dimens. Syst. Nanostruct, 132, 114716 (2021); <https://doi.org/10.1016/j.physe.2021.114716>.
- [4] A.S. Sethulekshmi, J.S. Jayan, A. Saritha, K. Joseph, *Insights into the reinforcing ability and multifarious role of WS<sub>2</sub> in polymer matrix*, J. Alloys Compd, 876, 160107 (2021); <https://doi.org/10.1016/j.jallcom.2021.160107>.
- [5] A. Jacob, P. Kurian, A.S. Aprem, *Transport properties of natural rubber latex layered clay nanocomposites*, J. Appl. Polym. Sci., 108(4), 2623 (2008); <https://doi.org/10.1002/app.26615>.
- [6] L. Bokobza, *Multiwall carbon nanotube elastomeric composites: A review*, Polymer, 48(17), 4907 (2007); <https://doi.org/10.1016/j.polymer.2007.06.046>.
- [7] W. Bauhofer, J.Z. Kovacs, *A review and analysis of electrical percolation in carbon nanotube polymer composites*, Comp. Sci. Technol, 69 (10), 1486 (2009); <https://doi.org/10.1016/j.compscitech.2008.06.018>.
- [8] S. Makhno, O. Lisova, P. Gorbyk, Y. Shi, K. Ivanenko, Y. Sementsov, *Estimation of Percolation Threshold and Its Influence on the Properties of Epoxy Resin-Based Polymer Composite Materials Filled Carbon Fibers and Carbon Nanotubes*, Springer Proceedings in Materials, 39 (2024); [https://doi.org/10.1007/978-981-97-1916-7\\_4](https://doi.org/10.1007/978-981-97-1916-7_4).
- [9] Y. Zare, *Study of nanoparticles aggregation/agglomeration in polymer particulate nanocomposites by mechanical properties*, Composites: Part A, 84, 158 (2016); <http://dx.doi.org/10.1016/j.compositesa.2016.01.020>.
- [10] M. Malagù, M. Goudarzi, A. Lyulin, E. Benvenuti, A. Simone, *Diameter-dependent elastic properties of carbon nanotube-polymer composites: Emergence of size effects from atomistic-scale simulations*, Composites: Part B, 131, 260 (2017); <https://doi.org/10.1016/j.compositesb.2017.07.029>.
- [11] M. Cen-Puca, A. Oliva-Avilés, F. Avilés, *Thermoresistive mechanisms of carbon nanotube/polymer composites*, Physica E, 95, 41 (2018); <https://doi.org/10.1016/j.physe.2017.09.001>.
- [12] Y.I. Sementsov, S.N. Makhno, S.V. Zhuravsky, M.T. Kartel, *Properties of polyethylene-carbon nanotubes composites*, Chemistry, physics and technology of surface, 8(2), 107(2017); <https://doi.org/10.15407/hftp08.02.107>.
- [13] Y.I. Sementsov, M.T. Kartel, *The influence of small concentrations of carbon nanotubes on the structuralization in matrices of different nature*, Chemistry, physics and technology of surface, 10(2), 174(2019); <https://doi.org/10.15407/hftp10.02.174>.
- [14] F. Lozovyi, K. Ivanenko, S. Nedilko, S. Revo, S. Hamamda, *Thermal analysis of polyethylene + X% carbon nanotubes*, Nanoscale Research Letters, 11(1), 97(2016); <https://doi.org/10.1186/s11671-016-1315-y>.
- [15] T.G. Avramenko, N.V. Khutoryanskaya, S.M. Naumenko, K.O. Ivanenko, S. Hamamda, S.L. Revo, *Effect of carbon nanofillers on processes of structural relaxation in the polymer matrixes*, Springer Proceedings in Physics, 221, 293(2019); [https://doi.org/10.1007/978-3-030-17759-1\\_20](https://doi.org/10.1007/978-3-030-17759-1_20).
- [16] M.M.J. Treacy, T.W. Ebbesen, J.M. Gibson, *Exceptionally high Young's modulus observed for individual carbon nanotubes*, Nature, 381, 678 (1996); <https://doi.org/10.1038/381678a0>.
- [17] A.H. Barber, S.R. Cohen, H.D. Wagner, *Measurement of carbon nanotube-polymer interfacial strength*, Appl Phys Lett., 82(23), 4140(2003); <https://doi.org/10.1063/1.1579568>.
- [18] K. Mylvaganam, L. C. Zhang, *Chemical Bonding in Polyethylene-Nanotube Composites: A Quantum Mechanics Prediction*, J. Phys. Chem. B., 108(17), 5217(2004); <https://doi.org/10.1021/jp037619i>.
- [19] S. Tretiak, *Triplet state absorption in carbon nanotubes: A TD-DFT study*, Nano Lett., 7(8), 2201(2007); <https://doi.org/10.1021/nl070355h>.
- [20] M.G. Ahangari, A. Fereidoon, M.D. Ganji, *Density functional theory study of epoxy polymer chains adsorbing onto single-walled carbon nanotubes: electronic and mechanical properties*, J Mol. Model., 19, 3127(2013); <http://dx.doi.org/10.1007/s00894-013-1852-6>.
- [21] V.V. Ivanovskaya, A.L. Ivanovsky, *About some directions of computer materials science of inorganic nanostructures*, Mathematical physics and modelling, 1(1), 7(2009).
- [22] Q. Zhang, X. Zhao, G. Sui, X. Yang, *Surface sizing treated MWCNTs and Its effect on the wettability, interfacial interaction and flexural properties of MWCNT/epoxy nanocomposites*, Nanomaterials, 8(9), 680(2018); <https://doi.org/10.3390/nano8090680>.
- [23] A.V. Melezhik, Y.I. Sementsov, V.V. Yanchenko, *Synthesis of fine carbon nanotubes on coprecipitated metal oxide catalysis*, Russian Journal of Applied Chemistry, 78(6), 917(2005); <https://doi.org/10.1007/s11167-005-0420-y>.
- [24] T.M. Pinchuk-Rugal, O.P. Dmytrenko, M.P. Kulish, Y.Y. Grabovskyy, O.S. Nychyporenko, Y.I. Sementsov, V.V. Shlapatskaya, *Radiation damages of isotactic polypropylene nanocomposites with multi-walled carbon nanotubes*, Problems of Atomic Science and Technology, 96(2), 10(2015).
- [25] A. Patterson, *The Scherrer formula for X-Ray particle size determination*. Phys. Rev., 56(10), 978 (1939); <https://doi.org/10.1103/PhysRev.56.978>.

- [26] S.M. Makhno, O.M. Lisova, R.V. Mazurenko, P.P. Gorbyk, K.O. Ivanenko, M.T. Kartel, Yu.I. Sementsov, *Electrophysical and strength characteristics of polychlorotrifluoroethylene filled with carbon nanotubes dispersed in graphene suspensions*, Applied Nanoscience, 13(12), 7591(2023); <https://doi.org/10.1007/s13204-023-02902-6>.
- [27] M.W. Schmidt, K.K. Baldrige, J.A. Boatz, S.T. Elbert, M.S. Gordon, J.H. Jensen, S. Koseki, N. Matsunaga, K.A. Nguyen, S. Su, T.L. Windus, M. Dupui, J.A.Jr. Montgomery, *General atomic and molecular electronic structure system*, J. Comput. Chem., 14(11), 1347(1993); <https://doi.org/10.1002/jcc.540141112>.
- [28] A.D. Becke, *Density functional thermochemistry. III. The role of exact exchange*, J. Chem. Phys., 98(7), 5648(1993); <https://doi.org/10.1063/1.464913>.
- [29] C. Lee, W. Yang, R.G. Parr, *Development of the Colle-Salvetti correlation-energy formula into a functional of the electron density*, Phys. Rev. B., 37(2), 785(1988); <https://doi.org/10.1103/PhysRevB.37.785>.
- [30] K. Jackson, S.K. Jaffar, R.S. Paton, *Computational Organic Chemistry*, Annu. Rep. Prog. Chem., Sect. B: Org. Chem., 109, 235(2013); <https://doi.org/10.1039/c3oc90007j>.
- [31] G.R. Hutchison, M.A. Ratner, T.J. Marks, *Intermolecular charge transfer between heterocyclic oligomers. effects of heteroatom and molecular packing on hopping transport in organic semiconductors*, J. Am. Chem. Soc. 127(48), 16866(2005); <https://doi.org/10.1021/ja0533996>.
- [32] S. Grimme, S. Ehrlich, L. Goerigk, *Effect of the damping function in dispersion corrected density functional theory*, J Comput Chem., 32(7), 1456(2011); <https://doi.org/10.1002/jcc.21759>.
- [33] S. Grimme, *Density functional theory with London dispersion corrections*, WIREs Comput. Mol. Sci., 1(2), 211(2011); <https://doi.org/10.1002/wcms.30>.
- [34] A.I. Alrawashdeh, J.B. Lagowski, *The role of the solvent and the size of the nanotube in the non-covalent dispersion of carbon nanotubes with short organic oligomers – a DFT study*, RSC Adv., 8, 30520 (2018); <https://doi.org/10.1039/C8RA02460J>.
- [35] D.J. Wales, R.S. Berry, *Limitations of the Murrell-Laidler Theorem*, J. Chem. Soc. Faraday Trans., 88, 543 (1992); <https://doi.org/10.1039/FT9928800543>.
- [36] S.F. Sun, *Physical Chemistry of Macromolecules: Basic Principles and Issues*. 2nd ed. (New York: Wiley, 2004).
- [37] T.P. Lodge, M. Muthukumar, *Physical chemistry of polymers: entropy, interactions, and dynamics*. J. Phys. Chem., 100(31), 13275 (1996); <https://doi.org/10.1021/jp960244z>.
- [38] Y. Yang, X. Ding, M.W. Urban *Chemical and physical aspects of self-healing materials*, Prog. Polym. Sci., 49–50, 34(2015); <https://doi.org/10.1016/j.progpolymsci.2015.06.001>.
- [39] S. Nikmatin, A. Syafiuddin, A.B. Hong Kueh, A. Maddu, *Thermal, and Mechanical Properties of Polypropylene Composites Filled with Rattan Nanoparticles*, Physical, J. Appl. Polym. Sci. Technol., 15(4), 386(2019); <https://doi.org/10.1016/j.jart.2017.03.008>.
- [40] A. Niemczyk, K. Dziubek, B. Sacher-Majewska, K. Czaja, M. Dutkiewicz, B. Marciniak, *Study of Thermal Properties of Polyethylene and Polypropylene Nanocomposites with Long Alkyl Chain-Substituted POSS Fillers*, J. Therm. Anal. Calorim., 125, 1287(2016); <https://doi.org/10.1007/s10973-016-5497-4>.
- [41] M.L. Minus, H.G. Chae, S. Kumar, *Polyethylene crystallization nucleated by carbon nanotubes under shear*, ACS Appl. Mater. Interfaces, 4(1), 326(2012); <https://doi.org/10.1021/am2013757>.
- [42] T. McNally, P. Potschke, P. Halley, M. Murphy, D. Martin, S.E.J. Bell, G.P. Brennan, D. Bein, P. Lemoine, J.P. Quinn, *Polyethylene multiwalled carbon nanotube composites*, Polymer, 46(19), 8222 (2005); <https://doi.org/10.1016/j.polymer.2005.06.094>.
- [43] O.S. Nychyporenko, O.P. Dmytrenko, M.P. Kulish, T.M. Pinchuk-Rugal, Y.Y. Grabovskyy, A.M. Zabolotnyy, V.V. Strelchuk, A.S. Nikolenko, Y.I. Sementsov, *Defects of structure of nanocomposites of polytetrafluorethylene with multiwalled carbon nanotube*, Nanosystems, Nanomaterials, Nanotechnologies, 13(4), 673(2015).
- [44] S. Kirkpatrick, *Rev Modern Phys.*, *Percolation and Conduction* 45, 574 (1973); <https://doi.org/10.1103/RevModPhys.45.574>.
- [45] A.L. Efros, *Physics and geometry of disorder* (Moscow: Nauka, 1982).
- [46] Y.P. Mamunya, *Electrical and thermal conductivity of polymer composites with dispersed fillers*, Ukrainian Chemistry Journal, 66(3), 55(2000). [in Ukrainian].
- [47] A. Quivy, R. Deltour, A.G.M. Jansen, P. Wyder *Transport phenomena in polymer-graphite composite materials*, Phys. Rev. B., 39(2), 1026(1989); <https://doi.org/10.1103/PhysRevB.39.1026>.
- [48] I. Balberg, N. Binenbaum, S. Bozovsky, *Anisotropic percolation in carbon black-polyvinylchloride composites*, Sol St Comm., 47(12), 989(1983); [https://doi.org/10.1016/0038-1098\(83\)90984-5](https://doi.org/10.1016/0038-1098(83)90984-5).
- [49] M.O. Lisunova, Y.P. Mamunya, N.I. Lebovka, A.V. Melezhyk, *Percolation behaviour of ultrahigh molecular weight polyethylene/multi-walled carbon nanotubes composites*, European Polymer Journal, 43(3), 949 (2007); <https://doi.org/10.1016/j.eurpolymj.2006.12.015>.
- [50] Y. Sementsov, X. Zhang, Kan. Kan, *Expanded Graphite and Its Composites* (Heilongjiang: Heilongjiang People's Publishing House, 2021).
- [51] J.C. Halpin, J.L. Kardos, *The Halpin-Tsai equations: A review*, Polym. Eng. Sci., 16(5), 344 (1976); <https://onlinelibrary.wiley.com/doi/pdf/10.1002/pen.760160512>.
- [52] A. Haque, A. Ramasetty, *Theoretical study of stress transfer in carbon nanotubes reinforced polymer matrix composites*, Composite Structures, 71(1), 68(2005); <https://doi.org/10.1016/j.compstruct.2004.09.029>.



- [53] M. Kartel, Y. Sementsov, S. Mahno, V. Trachevskiy, WangBo, *Polymer Composites Filled with Multiwall Carbon Nanotubes*, *Universal Journal of Materials Science*, 4(2), 23 (2016); <http://dx.doi.org/10.13189/ujms.2016.040202>.
- [54] Y.I. Sementsov, S.M. Makhno, S.V. Zhuravsky, M.T. Kartel, Himia, *Properties of polyethylene-carbon nanotubes composites*, *Fizika ta Tehnologia Poverhni*, 8(2), 107(2017); <https://doi.org/10.15407/hftp14.04.534>.

Ю. І. Семенцов<sup>1,2</sup>, Хао Тан<sup>1</sup>, Донгсін Ван<sup>1</sup>, Є.М. Дем'яненко<sup>2</sup>, М.І. Терещь<sup>2</sup>, К.О. Іваненко<sup>1,3</sup>, О.М. Ігнатенко<sup>2</sup>, С.М. Махно<sup>1,2</sup>, Н.В. Сігарьова<sup>2</sup>, С.В. Журавський<sup>2</sup>, Ю.В. Гребельна<sup>1</sup>, О.А. Чернюк<sup>2</sup>, М.Т. Картель<sup>2</sup>

## **Системи поліетилен та поліпропілен - нанонаповнювачі ВНТ: квантово-хімічне моделювання та експериментальні характеристики**

<sup>1</sup>*Нінбо Китайсько-український інститут промислових технологій нових матеріалів, район Чженхай, Нінбо, Китай*

<sup>2</sup>*Інститут хімії поверхні ім. О. О. Чуйка НАН України, Київ, Україна, [microft2@ukr.net](mailto:microft2@ukr.net)*

<sup>3</sup>*Інститут хімії високомолекулярних НАН України, Київ, Україна*

Метою роботи було експериментально та методами квантової хімії дослідити взаємодію графеноподібних нанокластерів з фрагментами полімерів тієї ж природи, але дещо іншої будови, на прикладі поліетилену (ПЕ) та поліпропілену (ПП). Експериментально показано, що армування ПЕ і ПП вуглецевими нанотрубками (ВНТ) шляхом перемішування в розплаві, попередньо розподіленими зі стабільної водної дисперсії на поверхні полімерного порошку, призводить до зміни структурно-механічних і термодинамічних характеристик. Змінюється ступінь кристалічності, розмір області когерентного розсіювання (ОКР), зростає напруження руйнування, деформація руйнування, змінюються термодинамічні характеристики, причому такі зміни характеристик для системи ПП-ВНТ переважають у порівнянні з системою ПЕ-ВНТ.

Розраховано енергію взаємодії графеноподібних фрагментів з олігомерами ПЕ та ПП. Встановлено, що енергія взаємодії графеноподібного нанокластера з поліпропіленовим олігомером є більшою, порівняно з поліетиленовим, що узгоджується з експериментальними даними щодо температур плавлення чистих полімерів та полімерних композитів з нанотрубками. Полімер з поверхнею нановуглецевого фрагмента утворює міжмолекулярний комплекс, який не є ковалентно зв'язаним, а утримується міжмолекулярними дисперсійними силами.

**Ключові слова:** нанокompозит, вуглецева нанотрубка, поліетилен, поліпропілен, метод теорії функціоналу густини, дисперсійні сили взаємодії.